Research Article

Orthogonal Wavelet Transform-Based Gaussian Mixture Model for Bearing Fault Diagnosis

Weipeng Li [iD],[1,2] Yan Cao [iD],[1] Lijuan Li [iD],[1] and Siyu Hou [iD][1]

[1]*School of Mechanical Electrical Engineering, Xi'an Technological University, Xi'an 710000, China*
[2]*School of Intelligent Manufacturing, Nanyang Institute of Technology, Nanyang 473000, China*

Correspondence should be addressed to Yan Cao; caoyan@xatu.edu.cn

The Gaussian mixture model (GMM) is an unsupervised clustering machine learning algorithm. This procedure involves the combination of multiple probability distributions to describe different sample spaces. Principally, the probability density function (PDF) plays a paramount role by being transformed into local linear regression to learn from unknown f failure samples, revealing the inherent properties and regularity of the data, and enhancing the subsequent identification of the operating status of the machine. The wavelet transform is a multiresolution transformation that can observe the signal gradually from coarse to fine, highlighting the localization analysis of nonstationary signals. Orthogonal wavelet transform selects the appropriate orthogonal wavelet function to transform so that the local characteristics of the signal in the time domain and frequency domain can be specifically described and the feature information of the original data can be mastered more effectively. In this study, a diagnostic method based on the Gaussian mixture model (OWTGMM) of orthogonal wavelet transform is proposed, in which orthogonal wavelet transform (OWT) is used to extract each detailed fault signal, the signal peak-to-peak value eigenvector is used as the construction model, and the GMM is used for fault classification. Based on the classification result from the rolling bearings' test data, the use of detail signals extracted through OWT as the training data of the Gaussian mixture model promotes fast classification of bearing faults. Compared with the GMM without the extraction of the characteristic values, this method can reliably distinguish the categories of bearing faults about 100% of the time, which is consistent with the service life test chart. Furthermore, the unknown fault data is subject to classification with the orthogonal wavelet Gaussian model, and the bearing fault data is well distinguished, with an overall recognition rate of over 95%.

1. Introduction

In recent years, the rapid development of machine learning algorithms has been widely used in the field of intelligent manufacturing, which also promotes the development of fault diagnosis and identification technology for rotating mechanical bearings, provides a scientific basis for production practice and management of rotating mechanical equipment, and promotes the core health management (PHM) system with prediction technology as its core. In "unsupervised learning" [1], the label information of training samples is unknown. The goal is to reveal the inherent nature and relationships in the data set through the learning of the unlabeled training sample which provides a reliable framework for further data analysis. In this category of learning, "clustering" is the most studied and extensively used [2]. GMM is one of the most successful clustering methods for modeling and can be used in both fault diagnosis and classification. In GMM, K (basically 3 to 5) Gaussian models are used to characterize the characteristics of fault data. After obtaining the characteristics, GMM is updated, and the currently extracted data characteristics are matched with GMM. Two parameters, the variance and the mean of the data in the whole Gaussian model play a decisive role. It is crucial to improve the learning ability of the mean and variance, and the choice of learning mechanism directly affects the stability, accuracy, and convergence of the model. To enhance the learning ability of the model, different

learning rates are adopted for the mean and variance in the improved method to improve the data classification and prediction effect in busy scenarios [3, 4]. Therefore, not only does the adoption of appropriate signal extraction methods accurately capture the characteristic information contained in the signals but it also reduces the data dimension significantly, thereby enabling GMM to quickly and accurately produce the diagnosis result.

A new tool wear state monitoring method, an entropy-based bearing defect spareness detection method, a sparse map of the sensitive filter band of an axial piston pump, and an entropy-based bearing detection method are studied [5, 6]. Numerical simulation and personalized diagnosis methods are used for detecting gear faults and the one-dimensional convolutional neural network, and the rolling-bearing fault diagnosis algorithm of INPSO-SVM have all been used in the rotating mechanical fault diagnosis neighborhood [7, 8]. Numerical simulation and finite element simulation is used to detect several fault diagnosis methods of bearings [9, 10]. Due to the presence of noise-free weak fault signals, the accuracy, effectiveness, and abnormal values are directly affected or caused by the fault diagnosis of rotating mechanical vibration. In predicting the service life of crucial bearing components [11], the extracted characteristics should reflect the operating status of the system, with the maintenance of high sensitivity to abnormal signals [12]. The feature extraction of noise-free weak fault signals is a big influencing factor in fault diagnosis. The wavelet transform is a signal processing method, which uses the extraction of each resolution. It is a branch of applied mathematics that began to rise in the late 1980s that achieves coarse-to-fine observation and demonstrates outstanding performance in the localized analysis of nonstationary signals [13, 14]. The orthogonal wavelet transform involves choosing an orthogonal wavelet function to transform, which can fully reflect the local characteristics of the time domain and frequency domain, thus enabling the effective and reliable comprehension of the characteristic information contained in the original data. Therefore, OWT [15, 16] and GMM [17, 18] are combined herein to form OWTGMM, and the construction method is given [19, 20]. In the application of OWTGMM in fault diagnosis, the orthogonal wavelet transform is used to extract the hierarchical features of the vibration signal and then extract the peak-to-peak feature signal as the training samples of the GMM to train the GMM classifier. The classification result of rolling bearings' test data shows that OWTGMM can enable fast classification of bearing faults. Compared with GMM without extracting characteristic values, the effectiveness of OWTGMM is proven, which is consistent with the service life test chart of the bearing. Furthermore, a satisfactory effect is achieved in the classification of the unknown fault data [21].

2. Gaussian Mixture Model

GMM uses the Gaussian probability density function (normal distribution curve) for accurate quantification and decomposes the dataset into several models based on the Gaussian probability density function (normal distribution curve). The mixture model does not require information on the subdistribution of observed data for the estimation of its probability in the overall distribution.

2.1. Single GMM. When the sample random variable X is univariate, the probability density function of the Gaussian distribution is expressed as follows:

$$P(x \mid \theta) = \frac{1}{\sqrt{2\pi\sigma^2}} \exp\left(-\frac{(x-\mu)^2}{2\sigma^2}\right), \tag{1}$$

where μ is the mean of the data (expected), and the σ denotes the standard deviation.

When sample X is multidimensional data (multivariate), the Gaussian distribution follows the following formula:

$$P(x \mid \theta) = \frac{1}{(2\pi)^{D/2}|\sum|^{1/2}} \exp\left(-\frac{(x-\mu)^T \sum^{-1}(x-\mu)}{2}\right), \tag{2}$$

where μ is the mean of the data (expected); $\sum$ is the covariance; and D signifies the dimension of the data.

2.2. GMM. The GMM can be considered to be a model comprising K single Gaussian models. The GMM is adopted in this study due to its satisfactory mathematical properties and computational performance.

First, the following is defined:

x_j is the observation sample, j = 1, 2, ..., N.

k is the number of central Asian Gaussian models representing the mixed model, k = 1, 2, ..., K.

α_k belongs to the kth submodel

$$\alpha_k \geq 0, \sum_{k=1}^{K} \alpha_k = 1. \tag{3}$$

$\phi(x \mid \theta_k)$ is the kth submodel for the Gaussian probability density function, $\theta_k = (\mu_k, \sigma_k^2)$. Its expansion is the same as the single Gaussian model introduced above.

γ_{jk} belongs to the kth submode for the probability that the jth observation data.

The probability distribution of GMM is as follows:

$$P(x \mid \theta) = \sum_{k=1}^{K} \alpha_k \phi(x \mid \theta_k). \tag{4}$$

For this model, $\theta = (\widetilde{\mu_k}, \widetilde{\sigma_k}, \widetilde{\alpha_k})$.

In modeling, some parameters such as variance, mean, and weights in the GMM should be initialized. With these parameters, the requisite data such as martensitic distance for modeling can be solved. During initialization, the variance is set as large as possible, while the weight is as small as possible (such as 0.001). This is because the initialized Gaussian model is an inaccurate possible model whose range should be constantly narrowed to update the parameters. By

setting a larger variance, we can include as many pixels as possible in a model to obtain the most likely model.

3. Orthogonal Wavelet Transformations

3.1. The Basic Concept of the Wavelet Transform.
A wavelet is a family of functions produced by a satisfied function $\int \varphi(t)dt = 0$ through translation and scaling.

$$\varphi_{a,b}(t) = |a|^{1/2}\varphi\left(\frac{t-b}{a}\right), a, b \in R, a \neq 0. \tag{5}$$

$f(t) \in L^2(R)$ for any function $f(t)$ is satisfied if $f(t) \in L^2(R)$. The continuous wavelet transform of the function $f(t)$ (continuous wavelet transform, CWT) is defined as follows:

$$\int f(t)\varphi_{a,b}^*(t)dt = 0, a \neq 0, \tag{6}$$

where $*$ represents the conjugation.

The function $\varphi(t)$ meets the following conditions [22, 23]:

$$C_\varphi = \int_{-\infty}^{+\infty} \frac{|\hat{\varphi}(\omega)|}{|\omega|}d\omega < +\infty, \tag{7}$$

when the function $f(t)$ ideally recovers

$$f(t) = \frac{1}{C_\varphi}\int\int_R^W \frac{f^{(a,b)}\varphi_{a,b}^*(t)}{a^2}da\,db. \tag{8}$$

Equation (8) is called the inverse transformation of the continuous wavelet transform.

Continuous wet transformation needs to be discretized in practical applications, especially in computers. The discretization here is for the continuous scaling parameters a and the continuous translation parameters b, not for time t.

3.2. Orthogonal Wavelet Overview.
The orthogonal wavelet transform aims to select the most appropriate orthogonal wavelet function for the transform, to specifically describe the local characteristics of the signal in the time domain and frequency domain, and to grasp the characteristic information of the original data more effectively.

3.2.1. The Haar wavelet.
Given the definition of serv the Haar wavelet, the scale function $\phi(t)$ of the Haar wavelet, i.e.,

$$\psi(t) = \begin{cases} 1, & 0 \leq t < 1/2, \\ -1, & 1/2 \leq t < 1, \\ 0, & \text{other}, \end{cases} \tag{9}$$

$$\varphi(t) = \begin{cases} 1, & 0 \leq t < 1, \\ 0, & \text{other}. \end{cases}$$

The integer displacements of $\psi(t)$ do not overlap with each other and $\langle\psi(t-k),\psi(t-k')\rangle = \delta(k-k')$ are orthogonal. in like manner, $\langle\psi_{j,k}(t),\psi_{j,k'}(t)\rangle = \delta(k-k')$.

Haar wavelet is limited and supported in the time domain and has an excellent positioning function. However, because the discontinuity of the time domain causes an infinite expansion of the frequency domain, its positioning function in the frequency domain is extremely poor, or its resolution is extremely poor.

3.2.2. Shannon wavelet.
A surname

$$\varphi(t) = \frac{\sin\pi t}{\pi t}, \tag{10}$$

$$\Phi(\omega) = \begin{cases} 1, & |\omega| \leq \pi, \\ 0, & \text{other}, \end{cases} \tag{11}$$

owing to

$$\langle\phi(t-k),\phi\left(t-k'\right)\rangle = \frac{1}{2\pi}\int\Phi_{0,k}(\omega)\Phi_{0,k}^*(\omega)d\omega = \frac{1}{2\pi}\int_{-\pi}^{\pi}e^{-j(k-k')\omega}d\omega = \delta\left(k-k'\right). \tag{12}$$

So the orthogonal $\{\varphi(t-k), k \in Z\}$ in the composition V_0 is one base. $\phi(t)$ is called the Shannon wavelet.

Since, $\phi_{0,k}(t) \in V_0$ and $V_0 \oplus W_0 = V_{-1}$ are of the two-scale nature and $\phi(2t-k) \in V_1$, thus

$$\Phi_{-1,k}(\omega) = \begin{cases} 1, & |\omega| \leq 2\pi, \\ 0, & \text{other}. \end{cases} \tag{13}$$

Yes $\psi(t) \in W_0$, if there is

$$\Psi(\omega) = \begin{cases} 1, & \pi < |\omega| \leq 2\pi, \\ 0, & \text{other}. \end{cases} \tag{14}$$

which can be found by

$$\psi(t) = \left(\frac{\sin\pi t/2}{\pi t/2}\right)\cos(3\pi t/2), \tag{15}$$

and can be easily to verified by

$$\langle\psi(t-k),\psi\left(t-k'\right)\rangle = \delta\left(k-k'\right). \tag{16}$$

That is $\{\psi(t-k), k \in Z\}$ the orthogonality in the composition W_0 of the same base. As depicted in the frequency domain, between $\Psi_{j,k}(\omega)$ and $\Phi_{j,k}(\omega)$ there is no overlap

with the respective and mutual integer shifts, so they are orthogonal.

The orthogonal wavelet shall be between Haar wavelet and Shannon wavelet, and the basic requirement of function $\psi(t)$ shall be bandpass; for $\int \psi(t)dt = 0$, it should be

oscillatory; $\Psi(\Omega)$ shall meet the tolerance conditions and the stability condition; moreover, $\Psi(\Omega)$ and $\Psi(\Omega)$ should preferably be tightly supported.

By the two-scale difference equation, $\Phi(\omega)$, $\Psi(\omega)$, $H_0(\omega)$, and $H_1(\omega)$ have an intrinsic connection.

$$\Phi(\omega) = \prod_{j=1}^{\infty} \frac{H_0\left(\omega/2^j\right)}{\sqrt{2}} = \prod_{j=1}^{\infty} H_0'\left(2^{-j}\omega\right),$$

$$\Psi(\omega) = \frac{H_1(\omega/2)}{\sqrt{2}} \prod_{j=2}^{\infty} \frac{H_0\left(\omega/2^j\right)}{\sqrt{2}} = H_1'\left(\frac{\omega}{2}\right) \prod_{j=2}^{\infty} H_0'\left(2^{-j}\omega\right).$$

(17)

These two equations explicitly state that the orthogonal wavelets and their scale function can generate [24, 25] by the infinite recurrence of the orthogonal filter set, as shown in Figure 1.

4. Intelligent Diagnosis and Evaluation Method of Bearing Fault

The orthogonal wavelet transformation mentioned above is adopted in the decomposition of the vibration signal, and the feature extraction is performed for corresponding local signals on each scale $f(t)$. The extracted peak-to-peak value of the local signals serves as the feature vector for the training of the OWTGMM. Then, the trained OWTGMM is used for intelligent classification and evaluation of bearing faults to achieve intelligent fault diagnosis [26]. OWTGMM specific algorithm program is as shown in Figure 2:

Step 1. The raw bearing signal is extracted, the features are extracted using the orthogonal wavelet method, the corresponding local detail signal is transformed, and the corresponding local detail of the $f(t)$ is analyzed at all scales from V_0 to V_{m-1}. The analysis results are shown in Figure 3. Where, V_0 is the original signal.

Step 2. For the feature extraction of normal signals in Step 1, the peak-to-peak feature vectors of the first five layers are used. Set the corresponding peak-to-peak value of W_i ($i = 1, 2, ..., m-1$) as $Xpp(i) = \max(W_i) - \min(W_i)$, ($i = 1, 2, 3..., m-1$), and the T-structure of the feature vector is as follows:

$$T = [Xpp(1), Xpp(2), Xpp(3), Xpp(m-1)].$$

(18)

Step 3. The feature matrix T constructed in Step 2 was used as the model input sample for the GMM and the GMM classification model is constructed.

Step 4. Concerning the test samples, the OWT characteristic is used to decompose the signal, refine the useful information, and reflect the signal characteristics. Furthermore, the peak-to-peak value of each layer is extracted as a set of

test samples and classified using the OWTGMM model, thus distinguishing the status.

Step 5. The more concentrated the Gaussian line of the GMM within the contour line, the more accurate the classification and the better the classification effect.

5. Experimental Analysis

5.1. Experiment Conditions. We used the experimental data from the rolling bearing test stand to verify the reliability of the model and to further verify the effectiveness of OWTGMM as a model for bearing performance evaluation. The data is from XJTU-ST-bearing data [27]. According to the relevant description in the study of applications in bearing degradation [28, 29], the vibration signal of the bearing in the horizontal direction provides more valuable information than the vibration signal in the vertical direction, which can reflect the state of the bearing equipment. Therefore, the horizontal vibration signals are used for this experiment. Figure 3 depicts the experimental platform. The accelerated degradation test performed on the rolling bearings starts at a fixed speed. In the test experiment, when the amplitude of the horizontal or vertical vibration signal of the bearing exceeds A^{10} and reaches the maximum value, it is determined that the bearing has failed and the new bearing needs to be replaced in time, and then the test bearing life test is over. The tested bearing may have any type of failure during the entire test process such as an outer ring fracture, an outer ring fault, an inner ring fault, and a rolling part fault. The LDK UER204 rolling bearings were the models tested in this experiment. The signal of the acceleration sensor is continuously collected, set the sampling frequency of 25.6 kHz, a sampling time of 1.28 s, 32,768 sampling data points), and a sampling period of 1 min, and data of 3 different working conditions of bearing are recorded (see Table 1). The feature extraction of the data under three different working conditions collected in the rolling bearing life test is performed. The method is orthogonal wavelet; db 10 is selected by wavelet function; 5 layers are decomposed; the signals of layers 5 and 4 are extracted; and the peak value vector is used as the input vector of the
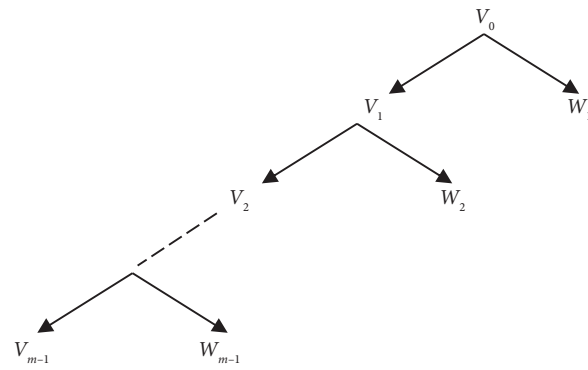
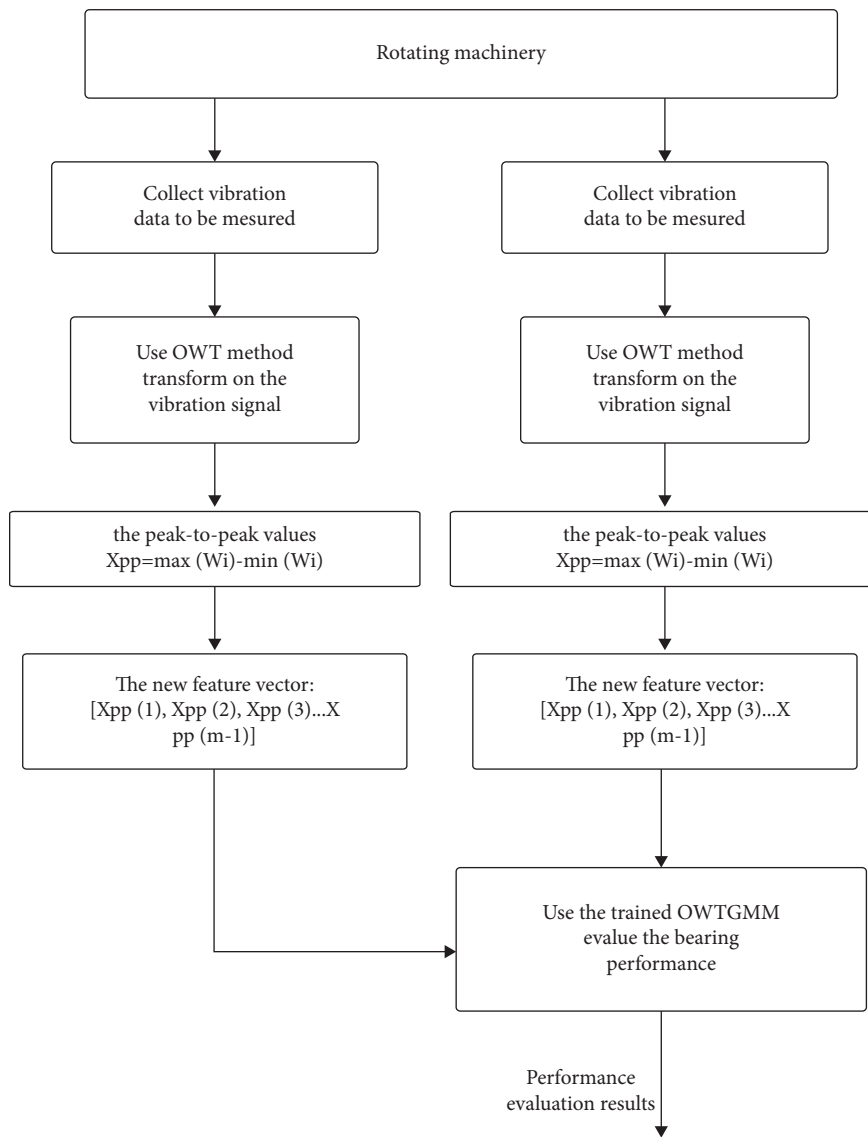FIGURE 1: The orthogonal wavelet and their scale functions.

FIGURE 2: Flows of performance degradation evaluation.

orthogonal wavelet The Gaussian mixture model (OWTGMM). The OWTGMM is trained with a set of constructed feature vectors.

The full-life data of bearing 1_5 under working condition 1 was used as the training modeling signal data. Experimental data of rolling bearing 1_5, signal acquisition
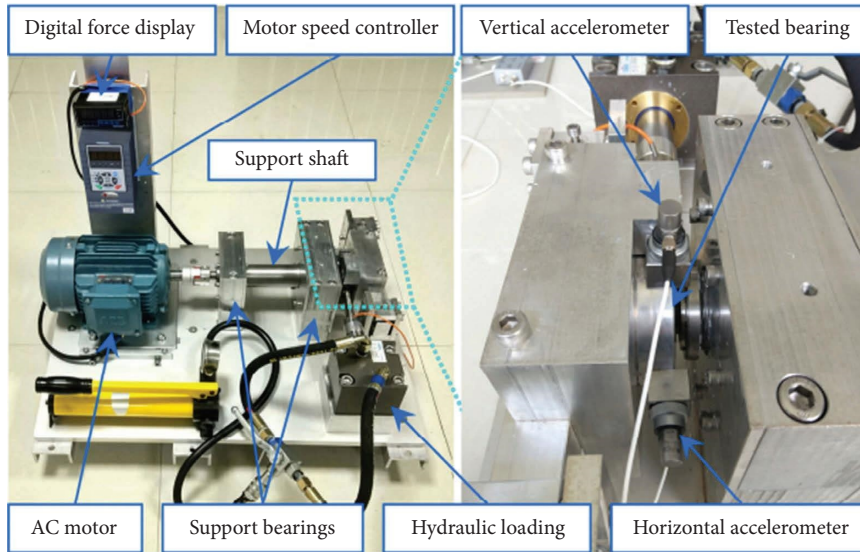
FIGURE 3: Accelerated life test-bed for bearing.

TABLE 1: Bearings operation condition.

Cutting condition	Spindle speed (rpm)	Radial force (kN)
Condition 1	2100	12
Condition 2	2250	11
Condition 3	2400	10

frequency of 25.6 kHz, acquisition time interval of 1 min, acquisition time length of 1.28 s, 52 groups of data samples, actual life of 52 minutes. The 5 sets of signal data are extracted for useful data, the data vector is used as the input vector of OWTGMM, and the OWTGMM model is established as the intelligent diagnosis of bearing fault diagnosis classifier. Figure 4 shows the time domain pattern of the full-life vibration data tested by the bearing 1_5 experimental bench. At the 35th time, the vibration amplitude of the rolling bearing increased significantly, which seriously deviated from the normal amplitude position. This is the beginning of the bearing degradation, and the RULE of the bearing is predicted.

5.2. Steps of Experiment

5.2.1. First, No Feature Extraction with OWT. No feature extraction is performed for every 100 sets of originally collected horizontal signal data at 6 min and 35 min, respectively. The 200 datasets are used as the input vector of the GMM classifier to test the classification of the fault signals. The test results are shown in Figure 5. The red dots represent the horizontal vibration fault data at 6 min, and the blue dots represent the *s* horizontal vibration fault data at 35 min. The figure shows that the fitted model differs considerably from the real data. Since GMM has only one center point, the two categories of fault data cannot be correctly classified, and the classification contours of the two datasets are not clear.

5.2.2. Second, Peak-to-Peak Feature Extraction of Data with OWT. The 200 datasets in Figure 5 are subject to OWT and decomposed into 5 layers, with db10 selected for this wavelet function. The detail signals of 5 and 4 layers were extracted, and the peak value feature vector was taken as the input data of the OWTGMM classifier, and the model was established for the intelligent classification of bearing fault data. The classification results are shown in Figure 6. The red dots represent the horizontal vibration fault data of the bearing at 6 min, and the blue dots represent the horizontal vibration fault data of the bearing at 35 min. The figure shows that the fitted model is very close to the real data distribution. The GMM has two central points, which represent the two Gaussian components, respectively. The two categories of fault data can be classified correctly, and the contour is clear and consistent with the two data categories.

5.2.3. Third, the OWTGMM Comparison of the Two Datasets. The orthogonal wavelet transformation is performed on the 100 sets of originally collected horizontal signal data at 6 min and the 200 sets of originally collected horizontal signal data at 35 min, respectively. They were decomposed into 5 layers, and db10 was selected for the wavelet function. The detail signals of the 5th and 4th layers were extracted, and the peak value of the feature vector was taken as the input data for the OWTGMM classifier, and the model was developed for the intelligent classification of the bearing fault data. The classification results are shown in Figure 7. The red dots represent the horizontal vibration fault data at 6 min, and the blue dots represent the horizontal bearing vibration fault data at 35 min. The figure shows that the two categories of fault data can be classified correctly, and the OWTGMM has two central points with clear contours. Subsequently, the same transformation is performed for the 100 sets of originally collected horizontal signal data at 6 min and 200
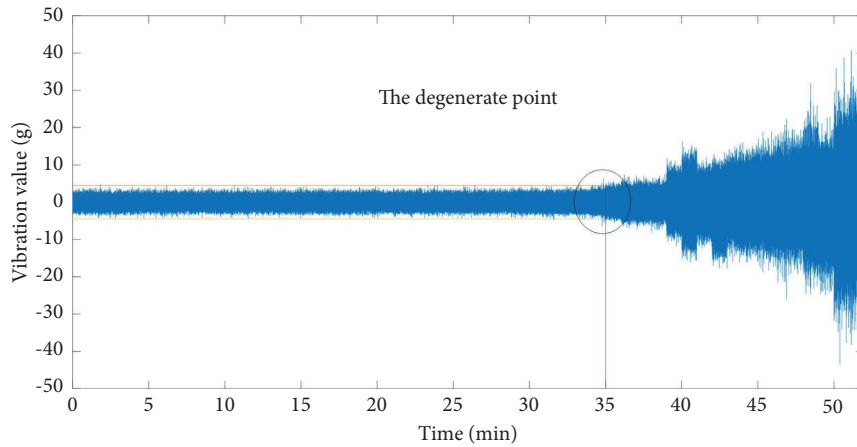
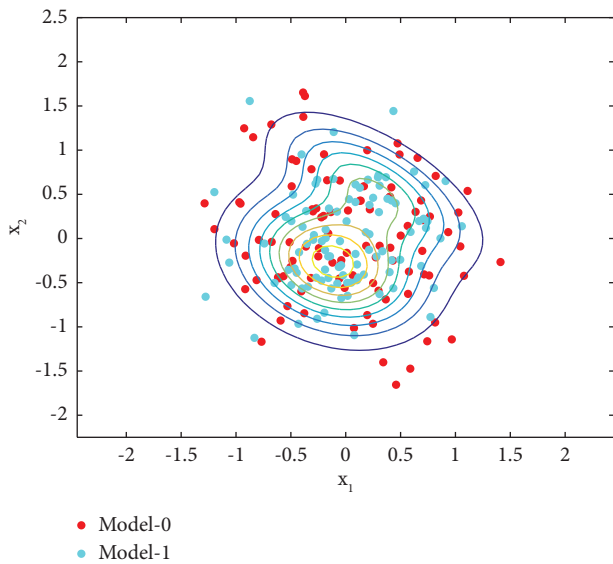FIGURE 4: Life cycle vibration signals of bearing 1_5.

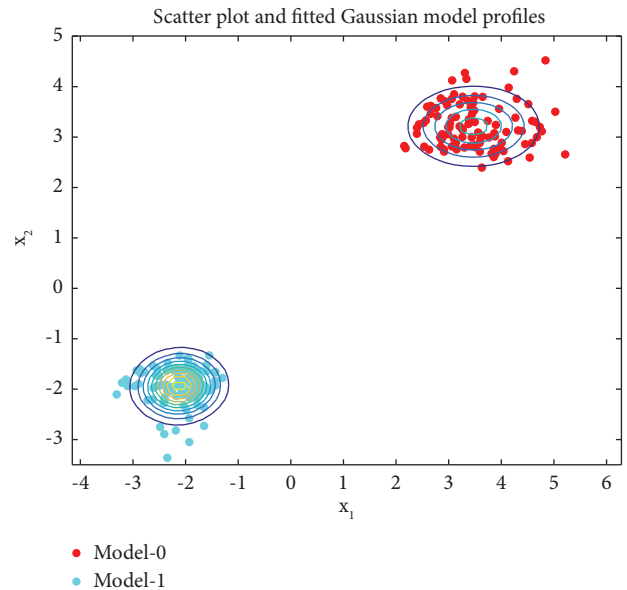FIGURE 5: GMM of horizontal vibration data of bearing at 6 min and 35 min.

FIGURE 6: OWTGMM of horizontal vibration data of bearing at 6 min and 35 min.

sets of originally collected horizontal signal data at 34 min, respectively. As the input data vector for the OWTGMM bearing fault intelligent classifier, the model is used to test the fault signal and perform intelligent classification. The Figure 8 shows that the central point of the OWTGMM is blurred with clear external contour and two central points cannot be formed, indicating that the performance of the bearing experiences considerable degradation after 34 min. Consistency with the time-domain analysis of the full-life vibration data of the bench bearing in Figure 4 illustrates the effectiveness of this method.

5.2.4. Fourth, the Membership Degree of the Two Fault Categories. In Figure 9, the red + represents the horizontal vibration fault data at 6 min, and the blue ○ means the horizontal vibration fault data at 35 min. The figure shows that the two data categories can be completely distinguished

and that the OWTGMM can achieve 100% classification accuracy. Then, the posterior probability and membership degrees of each set of fault data are calculated with OWTGMM, and the result is indicated with a color bar as shown in Figure 9. The closer it is to the red segment in the figure, the closer it is to the type 1 class. Conversely, the closer it is to the blue portion, the closer it is to type 2 class. In the figure, both the horizontal vibration fault data at 6 min, represented by red dots, and the horizontal vibration fault data at 35 min represented by blue dots are clearly marked. Therefore, the two datasets can be correctly classified with a high posterior probability.

5.2.5. Fifth, the Classification of the New Data with Trained OWTGMM. The 75 sets of unknown new bearings fault data collected at 10 min and 38 min are clustered with OWTGMM, and the observed results are shown in Figure 10. Red + means
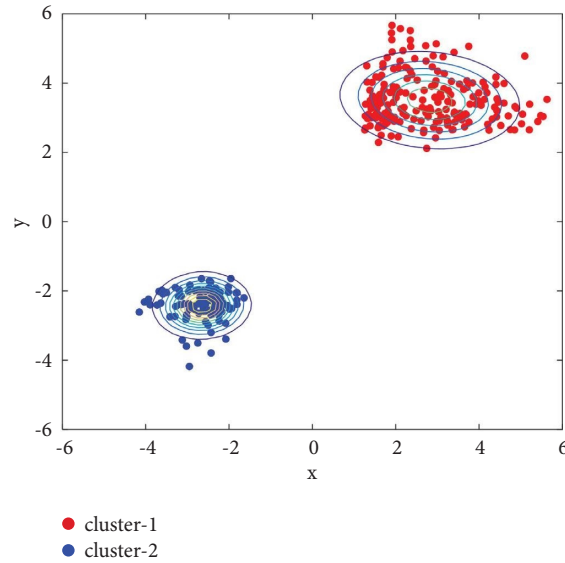
FIGURE 7: OWTGMM of bearing at 6 min (100 sets of data) and 35 min (200 sets of data).
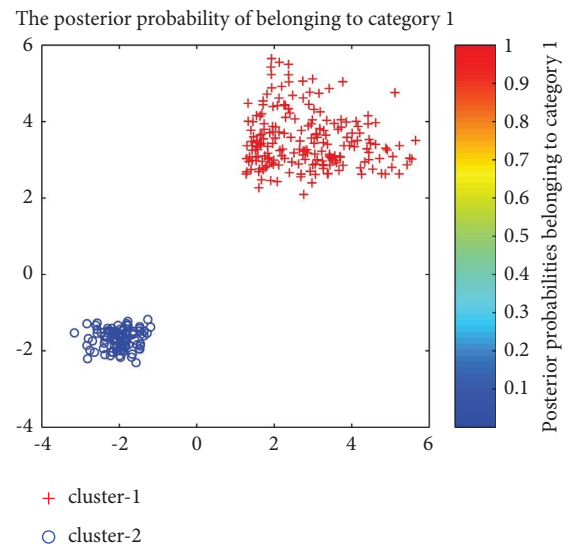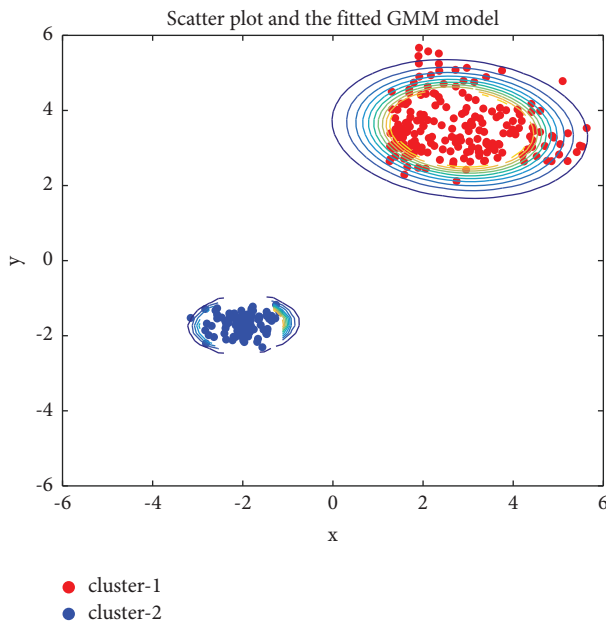

FIGURE 8: OWTGMM of bearing at 6 min (100 sets of data) and 34 min (200 sets of data).

FIGURE 9: Membership degree of the two types of fault.

the horizontal vibration fault sample at 10 min, and blue ○ means the horizontal vibration fault sample at 38 min. The figure shows that the data generated is correctly classified, with an overall recognition rate of over 95%.

5.2.6. *Finally, the Comparison of the OWTGMM Effect on Different Datasets.* The different bearing fault data were analyzed. Experimental data were obtained from the

Electrical Engineering Laboratory of Case Western Reserve University in the United States [30]. Normal bearing and inner load 0.007inc, the 2HP fault signal data was clustered with the OWTGMM generated in Figure 7 and the observed effect is shown in Figure 11. Red + represents the bearing horizontal vibration fault data, and the blue ○ represents the bearing horizontal vibration fault data. The figure on the left shows that the data generated is adequately classified with well-concentrated signals. The figure on the right shows that 5 blue faults are beyond the Gaussian line and 5 are on the Gaussian line, with an overall recognition rate of over 90%.
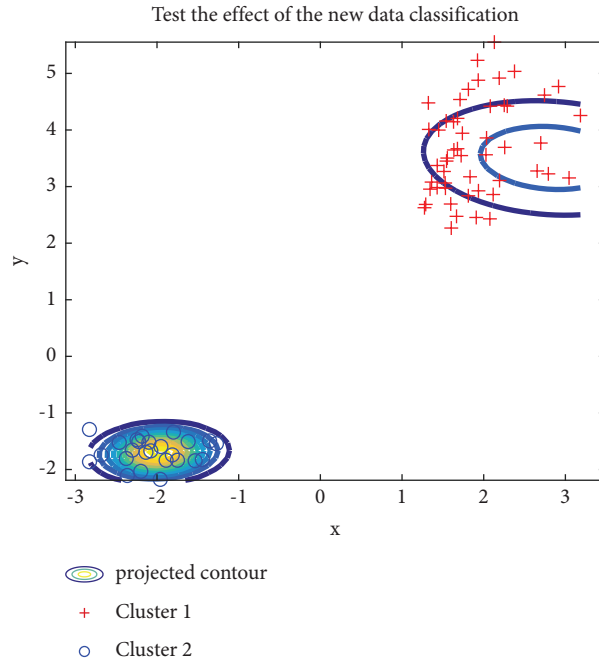
Test the effect of the new data classification

- ⬭ projected contour
- + Cluster 1
- ○ Cluster 2

FIGURE 10: Classification of new fault data with trained OWTGMM.

The posterior probability of belonging to category 1

- + cluster-1
- ○ cluster-2

Test the effect of the new data classification

- ⬭ projected contour
- + Cluster 1
- ○ Cluster 2

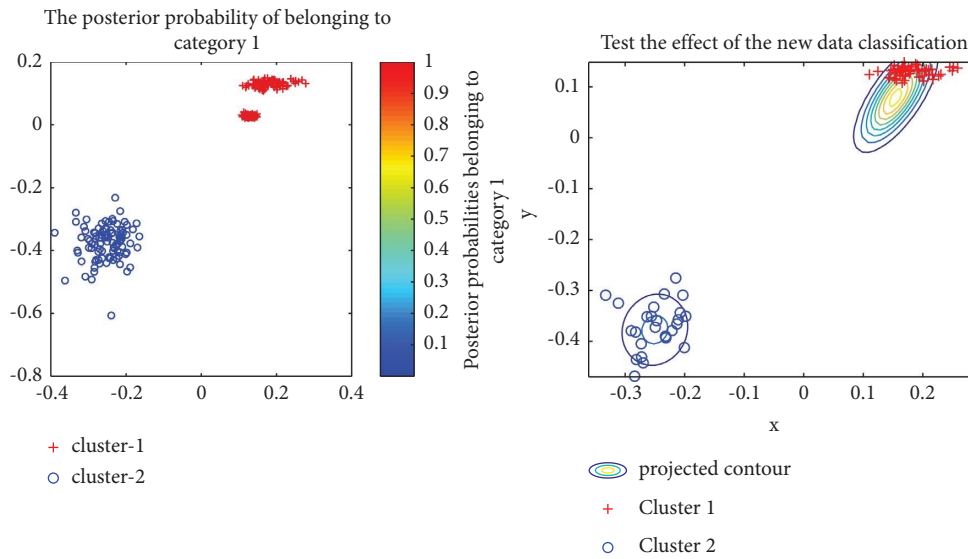FIGURE 11: OWTGMM comparison of different bearing fault data.

6. Conclusion

This paper proposes the combination of OWT and GMM to form an OWTGMM for the effective and efficient diagnosis of faulty bearing. In this method, bearing vibration signal decomposition through OWT, extract detailed useful signals, and input GMM to train the classification model. Then, the inherent properties and the laws governing the data are revealed through the learning of unlabeled training samples, thus ensuring fast-bearing fault classification. Compared with GMM, which does not use orthogonal wavelet function decomposition to extract detailed features, this method can distinguish bearing fault categories and achieve a high

recognition rate, which is consistent with the bearing full-life amplitude map. The findings from this experimental study suggest the following important conclusions:

(1) The GMM only has one central point for experimental data without the details extraction using orthogonal wavelet function decomposition. Hence, the two fault data cannot be reliably identified, and the classification boundaries are ambiguous.

(2) The GMM with feature extraction through orthogonal wavelet transformation has two central points which represent two Gaussian components, respectively. The two categories of fault data can be

classified correctly with clear contours and consistent effects.

(3) The comparison of the classification effects of the different datasets shows that the bearing performance undergoes considerable degradation after 35 min. The rapid performance degradation of the bearing at 35 min indicates that the vibration amplitude of the bearing fault increases rapidly, and the trend is consistent with the 100% change in fault amplitude of the bearing at 15 min in the full-vibration full-life test diagram of bearing 1_5.

(4) The two data categories have clear category marks and can be correctly classified with high posterior probabilities.

(5) The unknown fault data is clustered with OWTGMM. The bearing fault data is well distinguished, with an overall recognition rate of over 95%.

(6) Compared with the data set from the Electrical Engineering Laboratory of Case Western Reserve University in the United States, 90% of the classification diagnosis effect is achieved.

The orthogonal wavelet transform Gaussian hybrid model bearing fault diagnosis method (OWTGMM) is extensively adopted in the fields of bearing fault remote diagnosis, intelligent manufacturing, data cloud processing, and so on, which improves the bearing fault identification rate and data classification and processing efficiency. Subsequent studies will focus on the improvement of fault feature extraction technology and pattern recognition technology based on an acoustic signal, a thermal signal, and a deep vibration signal analysis. We will develop improved intelligent diagnosis methods based on the failure of various types of bearing equipment based on big data analysis.

Data Availability

The data used to support the findings of this study are available in this study.

Conflicts of Interest

The authors declare that they have no conflicts of interest.

Acknowledgments

References

[1] J. W. Han and M. Kamber, *Data Mining: Concepts and Techniques*, Machine Press, Beijing:China, 2000.

[2] D. Aloise, A. Deshpande, P. Hansen, and P. Popat, "NP-hardness of Euclidean sum-of-squares clustering," *Machine Learning*, vol. 75, no. 2, pp. 245–248, 2009.

[3] W. H. Pun and B. D. Jeffs, "Adaptive image restoration using a generalized Gaussian model for unknown noise," *IEEE Transactions on Image Processing*, vol. 4, no. 10, pp. 1451–1456, 1995.

[4] T. T. Pham and R. J. P. deFigueiredo, "Maximum likelihood estimatio of a class of nonuGausslan densities with application to ipdeconvolution[J]," *IEEE Transactions on Acoustics, Speech, & Signal Processing*, vol. 37, no. 1, pp. 73–82, 1989.

[5] Y. Zhou, G. Zhi, W. Chen, and I. Deng, "A new tool wear condition monitoring method based on deep learning under small samples[J]," *Measurement*, vol. 189, 2022.

[6] Z. Yuqing, K. Anil, P. Chander, and T. Shen, "A novel entropy-based sparsity measure for prognosis of bearing defects and development of a sparsogram to select sensitive filtering band of an axial piston pump [J]," *Measurement*, vol. 203, 2022.

[7] X. Liu, H. Huang, and J. A. Xiang, "Personalized diagnosis method to detect faults in gears using numerical simulation and extreme learning machine[J]," *Knowledge-Based Systems*, vol. 195, Article ID 105653, 2020.

[8] Y. Shao, X. Yuan, C. Zhang, Y. Song, and Q. Xu, "A novel fault diagnosis algorithm for rolling bearings based on one-dimensional convolutional neural network and INPSO-svm," *Applied Sciences*, vol. 10, no. 12, p. 4303, 2020.

[9] S. Yang, X. Yuan, C. Zhang, and X. Xiao, "A novel fault diagnosis algorithm for rolling bearings based on one-dimensional convolutional neural network and INPSO-svm," *IEEE/ASME Transactions on mechatronics*, vol. 27, p. 5, 2022.

[10] Y. Gao, X. Liu, and J. Xiang, "FEM simulation-based generative adversarial networks to detect bearing faults," *IEEE Transactions on Industrial Informatics*, vol. 16, no. 7, pp. 4961–4971, 2020.

[11] D. Y. Zeng, Y. L. Jiang, Y. S. Zou, and Y. Chen, "Construction and verification of a new evaluation index for bearing life prediction characteristics[J]," *Journal of Vibration and Shock*, vol. 40, no. 22, pp. 18–27, 2021.

[12] Y. L. Xu, M. Qiu, J. X. Li, and F. Zhang, "Remaining useful life prediction method of rolling bearing based on SKF- KF-Bay [J]," *Journal of Vibration and Shock*, vol. 40, no. 19, pp. 26–31+40, 2021.

[13] J. W. Jiang and Y. H. Hu, "Fault analysis of diesel engine based on wavelet packet feature extraction and fuzzy entropy feature selection [J]," *Journal of Vibration and Shock*, vol. 39, no. 4, pp. 273–277+298, 2020.

[14] X. B. iu, M. M. Zhang, J. C. Tu, and J. Feng, "Wavelet clustering algorithm based on breadth first search [J]," *Vibration and impact*, vol. 35, no. 15, pp. 178–183, 2016.

[15] Y. N. Pan and J. Chen, "Application of wavelet packet - support vector data description in performance degradation assessment of bearings [J]," *Journal of Vibration and Shock*, vol. 28, no. 4, pp. 164–167, 2009.

[16] X. B. Liu, Z. D. Han, W. Q. Shao, and H. Y. Zuo, "Double grid correction crossover wavelet clustering algorithm based on hash function [J]," *Journal of Vibration and Shock*, vol. 37, no. 21, pp. 267–272+280, 2012.

[17] Y. Song and F. L. Yin, *Research on the Motion Object Detection Algorithm Based on a Gaussian Hybrid model[D]*, Lanzhou University, Lanzhou, 2008.

[18] G. L. Sun and J. L. Tang, "Semi-supervised learning algorithm based on a hierarchical Gaussian hybrid model[J]," *Computer Research and Development*, vol. 41, no. 1, pp. 156–161, 2004.

[19] W. P. Li, Y. Cao, and L. J. Li, "Orthogonal wavelet transform KCA in fault diagnosis[J]," *Journal of Vibration and Shock*, vol. 40, no. 7, pp. 291–296, 2021.

[20] W. P. Li, Y. Cao, L. J. Li, and S. Hou, "An orthogonal wavelet transform-based K-nearest neighbor algorithm to detect faults

in bearings," *Shock and Vibration*, vol. 2022, pp. 1–13, Article ID 5242106, 2022.

[21] Y. Gao, X. Liu, H. Huang, and J. Xiang, "A hybrid of FEM simulations and generative adversarial networks to classify faults in rotor-bearing systems," *ISA Transactions*, vol. 108, pp. 356–366, 2021.

[22] W. P. Li, Y. Cao, and L. J. Li, "Orthogonal wavelet transform KCA in fault diagnosis[J]," *Journal of Vibration and Shock*, vol. 40, no. 7, pp. 291–296, 2021.

[23] S. Haidong, J. Hongkai, Z. Ke, W. Dongdong, and L. Xingqiu, "A novel tracking deep wavelet auto-encoder method for intelligent fault diagnosis of electric locomotive bearings," *Mechanical Systems and Signal Processing*, vol. 110, pp. 193–209, 2018.

[24] S. W. Li, D. L. Zhang, X. Y. Huang, and D. Chen, "Application of data feature selection and classification in mechanical fault diagnosis[J]," *Journal of Vibration and Shock*, vol. 39, no. 2, pp. 218–222, 2020.

[25] S. W. Li, D. L. Zhang, X. Y. Huang, and P. Chen, "Application of data feature selection and classification in mechanical fault diagnosis [J]," *Journal of Vibration and Shock*, vol. 39, no. 2, pp. 218–222, 2020.

[26] J. M. Zhu, "Wavelet transform and its engineering application (serial)[J]," *Vibration and Impact*, vol. 4, pp. 85–91, 1996.

[27] B. Wang, Y. Lei, N. Li, and N. Li, "A hybrid prognostics approach for estimating remaining useful life of rolling element bearings," *IEEE Transactions on Reliability*, vol. 69, pp. 401–412, 2020.

[28] A. Soualhi, K. Medjaher, and N. Zerhouni, "Bearing health monitoring based on Hilbert-huang transform, support vector machine, and regression," *IEEE Transactions on Instrumentation and Measurement*, vol. 64, no. 1, pp. 52–62, 2015.

[29] L. Guo, N. Li, F. Jia, Y. Lei, and J. Lin, "A recurrent neural network based health indicator for remaining useful life prediction of bearings," *Neurocomputing*, vol. 240, no. 3, pp. 98–109, 2017.

[30] L. J. Li, J. Han, W. P. Li, and L. Xia, "Applying orthogonal wavelet transform-SVDD to evaluating performance of bearing[J]," *Mechanical Science and Technology*, vol. 31, no. 7, pp. 1201–1204, 2012.